Applied Catalysis B: Environmental 91 (2009) 165–173

Contents lists available at ScienceDirect

Applied Catalysis B: Environmental

journal homepage: www.elsevier.com/locate/apcatb

Impact of the morphological properties of thin TiO_2 photocatalytic films on the detoxification of water contaminated with the cyanotoxin, microcystin-LR

Maria G. Antoniou [a], Persoulla A. Nicolaou [b], Jody A. Shoemaker [c], Armah A. de la Cruz [c], Dionysios D. Dionysiou [a,*]

[a] Department of Civil and Environmental Engineering, University of Cincinnati, Cincinnati, OH 45221-0071, USA
[b] Department of Pharmacology and Cell Biophysics, College of Medicine, University of Cincinnati, Cincinnati, OH 45267-0575, USA
[c] Office of Research and Development, U.S. Environmental Protection Agency, Cincinnati, OH 45268, USA

ARTICLE INFO

Article history:
Received 23 February 2009
Received in revised form 12 May 2009
Accepted 13 May 2009
Available online 21 May 2009

Keywords:
Cyanotoxins
Microcystin-LR
Photocatalytic
TiO_2 photocatalysis
Thin films
Water treatment
Water detoxification
PP1 enzyme

ABSTRACT

This study investigated the use of thin transparent TiO_2 photocatalytic films, prepared with novel sol–gel methods containing surfactants as templating materials, for the degradation of the cyanotoxin, microcystin-LR (MC-LR). MC-LR is an emerging contaminant from the Contaminant Candidate Lists (CCLs 1–3) of the USEPA. The effects of UV-A radiation, solution pH, initial toxin concentration, coated surface area of the TiO_2 films and their structural properties (porosity, crystallinity and thickness) on the degradation rate of MC-LR were investigated. Photolysis did not occur with UV-A radiation. Acidic pH was more efficient for the degradation of MC-LR due to toxin interaction with the catalyst surface and increased adsorption into the porous films. The degradation profiles of the toxin at different initial concentrations were fitted with *pseudo-first order* kinetics. Films prepared with three coatings (0.3 μm thickness) had the best performance at acidic and neutral pH, while the exclusion of surfactant from the preparation method resulted in non-porous films with decreased performance. The parameter that mostly affected the degradation rate was the solution pH. The toxicity of the treated samples, evaluated by an in-house protein phosphatase 1 assay, indicated that treatment with the TiO_2 photocatalytic films indeed resulted in complete removal of MC-LR's toxicity.

1. Introduction

Cyanotoxins are secondary metabolites produced and released by harmful strains of cyanobacterial algal blooms (also known as Cyano-HABs). Cyano-HABs drastically diminish water quality by producing undesirable color, taste and odor and releasing harmful cyanotoxins into the water. The occurrence of Cyano-HABs has become more prevalent globally as a direct consequence of increasing nutrient levels in surface waters, mainly caused by human activities (i.e., sewer runoffs, overuse of fertilizers) [1–3]. In fact, a study in Greece (1987–2000) confirmed that the warm waters of the Mediterranean sea favor the growth of toxic genera of *Microcystis spp.* with high intracellular concentrations of microcystins (a group of cyanotoxins that exhibit hepatotoxic activity) [4]. In China, persistent blooms in vital water bodies such as Lake Tai forced the environmental services to restrict water availability for 2 million people in Spring 2007 [5,6] and recent studies have correlated elevated levels of primary liver cancer in specific parts of China with microcystin exposure [7]. In addition, microcystins are considered to be the most important drinking water contaminant related to cyanobacteria in Southeastern Australia [8]. For these reasons, microcystin-LR (MC-LR), the most toxic and most frequently encountered derivative of the microcystin group, was chosen as a cyanotoxin-model contaminant in our current studies [9–11].

For the past decades, research has focused on finding effective technologies to address the removal of the cyanobacterial cells and/or the cyanotoxins contaminating vital water sources. Both conventional and chemical oxidation treatments have been tested to remove cyanobacteria and their toxins [1,12,13]. Since commonly used water treatment processes (i.e. coagulation, filtration) induce cyanobacteria cells to rupture, thereby releasing cyanotoxins in the finished water [14], advanced oxidation technologies (AOTs) are currently being considered to treat the soluble toxins [12]. TiO_2 photocatalysis is known to be among the most promising AOTs. It is a "green" technology, which generates reactive hydroxyl radicals ($HO^{\bullet}$) that readily react with organic compounds to efficiently perform water purification, disinfection and detoxification without utilizing or producing hazardous compounds [15,16]. TiO_2 is abundant in nature in the form of

* Corresponding author at: Department of Civil and Environmental Engineering, University of Cincinnati, 765 Baldwin Hall P.O. Box 210071 Cincinnati OH 45221-0071 United States. Tel.: +1 1513 556 0724; fax: +1 1513 556 2599.
E-mail address: dionysios.d.dionysiou@uc.edu (D.D. Dionysiou).

0926-3373/$ – see front matter © 2009 Elsevier B.V. All rights reserved.
doi:10.1016/j.apcatb.2009.05.020

nano-size particles that possess high surface area and porosity [15]. Titania has been used to photocatalytically treat contaminated water and air in systems involving direct irradiation of nanoparticles in a slurry form [17–20]. It has been stated that in order for TiO_2 photocatalysis to be adopted in water treatment trains, the catalyst must be immobilized on a substrate [19,21]. Therefore, herein, TiO_2 immobilized on films, was utilized for the degradation of cyanotoxins as an alternative to TiO_2 nanoparticles [22,23]. This methodology may be more efficient and practical as the immobilization of the catalyst on a substrate (i.e. glass, stainless steel and ceramic) eliminates the need for post-treatment removal of turbidity caused by nanoparticles, an important aspect as recent studies highlighted concerns about the possible toxicity of residual nanoparticles [24].

In our previous studies, we focused on the transformations that MC-LR undergoes following treatment with photocatalytic films [9–11]. Mass spectrometry (MS) was selected as the appropriate analytical tool for identifying the intermediates formed. Initially, the tandem MS (MS/MS) fragmentation patterns of the newly formed $[M+H]^+$ ions were recorded, followed by structural identification [10]. Consequently, the structures of the intermediates were elucidated, the degradation pathways were unveiled, and the preferential sites for degradation of MC-LR were reported [11].

In this study, we focused on the practical aspects of the application of these photocatalysts and the parameters that can influence their efficiency to degrade the cyanotoxin. It is well known that the three major steps that can affect the photocatalytic oxidation (PCO) of a contaminant are: (a) the transfer of the contaminant from the bulk to the surface of the titania, (b) the adsorption of the pollutant on the catalyst, and (c) the surface reaction with the $HO^{\bullet}$ [25]. Therefore, we investigated how the morphological properties of the catalyst (thickness, porosity, crystallinity, and surface area) combined with important water parameters (solution pH, initial toxin concentration) can affect the degradation of MC-LR and identify the rate-limiting step. A protein phosphatase inhibition enzyme assay was developed in-house to evaluate the toxicity of the treated samples. This knowledge can assist in adopting practices that elevate the performance of the photocatalytic films and provide insightful input for the suitable design of a large-scale reactor as well as the fate of the cyanotoxin following treatment.

2. Experimental

2.1. Safety

Cyanotoxins can cause acute, and chronic poisoning through inhalation, ingestion and skin exposure, respectively, therefore they need to be handled with extreme care. The toxin was handled with appropriate personal protective equipment while the experiments were conducted in an Advance SterilchemGARD III Class II Biological Safety Cabinet (The Baker Company, PO Box Drawer E, Sanford, ME 04073) with full exhaust.

2.2. Materials and methods

Solid MC-LR (0.5 mg) purchased from CalBiochem (96.4%; FW = 995.2 g/mole) was stored at −20 °C. A 482 mg/L standard of toxin solution was prepared by dissolving 0.5 mg of solid toxin with 1 mL of autoclaved Milli-Q® Synthesis A10 water (Millipore Corp., Billerica, MA USA; conductivity, 0.05 μS/cm). To achieve different toxin concentrations, specific aliquots (range of μL) of the 482 mg/L standard solution were spiked in pre-adjusted pH solutions, buffer solution or Milli-Q water. The quantification of the toxin was performed with an Agilent 1100 Series quaternary LC (liquid chromatograph) equipped with a photodiode array detector (PDA) set at 238 nm. A C_{18} Discovery HS (Supelco) column (4.6 mm × 150 mm, 3 μm particle size) was utilized as a stationary phase, while the mobile phase was a mixture of 0.05% (v/v) trifluoroacetic acid (TFA) in acetonitrile solution and 0.05% (v/v) TFA in Milli-Q water in 40:60 ratio. The analysis was conducted under isocratic conditions and MC-LR eluted at about 5.4 min. The flow rate was set at 1 mL/min and the injection volume was 50 μL. The temperature of the column was set at 40 °C. Details on the analytical methods (isocratic and gradient) as well as the operational parameters of the Thermo Finnigan LCQ Deca ion trap mass spectrometer are reported elsewhere [9–11]. The UV–Vis spectrum of MC-LR was obtained using a Spectramax M2 spectrophotometer (Molecular Devices Corp., Sunnyvale, CA).

2.3. Preparation of thin photocatalytic films

For the fabrication of TiO_2 thin films, TiO_2 sol comprised of titanium tetraisopropoxide, acetic acid, isopropanol and Tween 80 surfactant was coated on glass substrate and heat treated at 500 °C to remove the surfactant templates [22,23]. The dip-coating–calcination cycle was repeated 3 times for each film unless noted otherwise, resulting in uniform and transparent mesoporous nanocrystalline TiO_2 films with high surface area (147 m^2/g), porosity (46%) and small anatase crystallite size (9.2 nm). The amount of catalyst per cm^2 was estimated to be 62.2 $\mu g/cm^2$ based on the density of anatase TiO_2 (3.89 g/cm^2), the film thickness (0.3 μm) and the film porosity (46.2%). The overall coated area of each film (both sides) was 22.5 cm^2 (2.5 cm × 4.5 cm × 2).

2.4. Experimental setup

Thin film (or films) was placed in a sealed round (diameter = 10 cm) pyrex reactor vessel that contained 10 mL of MC-LR solution (of predetermined concentration and pH) and illuminated from the top with two long wave 15 W UV lamps (Cole-Parmer, λ_{max} = 365 nm). The intensity of the radiation measured with an IL 1700 Research Radiometer/Photometer (Inter National Light) was found to be 35 $\mu W/cm^2$ at 6 cm.

2.5. Inhibition studies-assay procedure

To determine the potential toxicity of the treated samples, we developed a colorimetric assay (λ = 405 nm) that measures alterations of the activity of the PP1 enzyme (0.1 mg/mL, New England Biolabs, Cat# P0780S). All solutions were freshly prepared. The assay buffer contained 20 mM Tris-HCl (Sigma, Cat# T5941), 0.1 mM $Na_2EDTA{\cdot}2H_2O$ (Sigma, Cat# E1644), 5 mM dithiothreitol, DTT (Sigma, Cat# D0632) and 1.0 mM of $MnCl_2$ (Fisher, Cat# M87-100) and the pH was adjusted to 7 with 0.1N NaOH (Fisher, Cat# 1310-73-2). The substrate, 4-nitrophenyl phosphate disodium salt hexahydrate, pNPP (Sigma, Cat# P4744) was dissolved in Milli-Q water to give a 40 mM solution. The PP1 enzyme was diluted with the assay buffer 40 times (0.0025 mg/mL). All the solutions were kept in an ice-bath for the duration of the assay. 10 μL of Milli-Q water (controls) or 10 μL of sample along with 40 μL of PP1 were added in each well of a 96-well microtiter plate (1/2 area flat bottom, Corning Inc, Cat # 3370) and then incubated at 37 °C for 5 min. A 50 μL aliquot of the substrate was added and further incubated at 37 °C. The progression of the reaction was monitored by taking readings of the color formation (λ = 405 nm) in a UV–vis spectrophotometer ($VERSA_{max}$ microplate reader, Molecular Devices) at 10 and 30 min after the substrate was added. Blank readings (which contained all the components of the assay but PP1 enzyme that was substituted with H_2O) were also taken. The optimum enzyme concentration was determined by performing

serial dilutions (up to 4 log) of 0.0025 mg/mL PP1 standard. The error bars represent the standard deviation of triplicates.

2.6. Statistical and structural analysis

GraphPad Prism 4 software was utilized for the statistical analysis of the experimental data. To investigate the effect of a film property such as thickness, global fitting was used. The comparison of three mean values (treatment points, initial rates) was conducted with one-way ANOVA combined with the Bonferroni's multiple comparison test as a post-test. The null hypothesis tested was that values are the same (H_o: $\mu_1 = \mu_2$) while the alternative was the values are different (H_a: $\mu_1 \neq \mu_2$). All the tests were two sided for $\alpha = 0.05$. The *ChemOffice 2002* software was used for drawing chemical structures and calculating the diameters of MC-LR and methylene blue (that was used to compare with MC-LR).

3. Results and discussion

3.1. Control experiments

To identify possible losses of the toxin, control experiments were performed to check the stability of the compound at neutral and acidic pH, the effect of UV-A radiation and the absorbance of the toxin on the catalyst (Fig. 1). The cyclic structure of MC-LR provides great stability to this compound and therefore, no loss was observed from volatilization or absorption on the glass reactor at neutral pH or acid hydrolysis of MC-LR at pH = 3.0. As seen from the UV–Vis spectra of MC-LR, no significant adsorption takes place at $\lambda = 365$ nm (Fig. 2) and since the maximum absorption of the toxin occurs at 238 nm, photolytic degradation with UV-A radiation was not observed. In addition, since the photolysis experiments were conducted in Milli-Q water in the absence of photosensitizers, such as humic acids [26], and pigments [27], the toxin concentration remained unaltered over time. When an acidic toxin solution (pH = 3.0) was in contact with the TiO_2 film for 4 h in the dark, approximately 50% of the toxin (C_o = 900 μg/L, ~0.9 μM), equal to 4.2 nmol, was removed by adsorption. At an estimated diameter between 1.2 and 2.6 nm [12], adsorption of MC-LR is favored in the mesoporous range. The thin transparent films used in this study have distinct pore structure averaging diameters of 3–7 nm and high porosity of 46.2% which favors the retention of MC-LR [22]. In addition, at acidic pH (more on the pH effect in a following section) attractive forces developed between the toxin and the catalyst assisting in the adsorption of the toxin onto the catalyst. However, the slow adsorption of MC-LR onto the films compared to nanoparticles [9,17–19] is attributed to mass transfer restrictions and the gradual availability of surface area for the adsorption of the toxin as it diffuses into the pores. To rule out the possibility of surface catalyzed processes under acidic pH in the dark, we performed dark adsorption of MC-LR at pH = 3.0 over a 24 h period and then increased the pH to Milli-Q water (pH_{sq} = 5.8) and after 4 h, increased the pH to basic (pH = 9.2) for another 24 h to see if we can recover the adsorbed toxin. After the first 30 min at pH_{sq} = 5.8, the initial toxin concentration was completely recovered. This eliminates the possibility of reduction of the concentration of the toxin because of degradation in the dark. The destruction of MC-LR occurred only when both the catalyst and radiation were present, with the toxin almost completely removed after 4 h of treatment with thin films (Fig. 1).

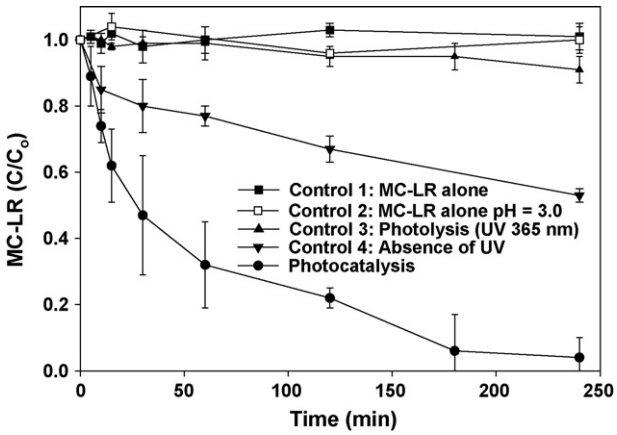

Fig. 1. Photocatalytic and control experiment of MC-LR (C_o~0.9 μM) with the thin films.

The overall mass of catalyst per film was approximately 1.4 mg-catalyst (62.2 μg/cm^2 × 22.5 cm^2), while studies with P-25

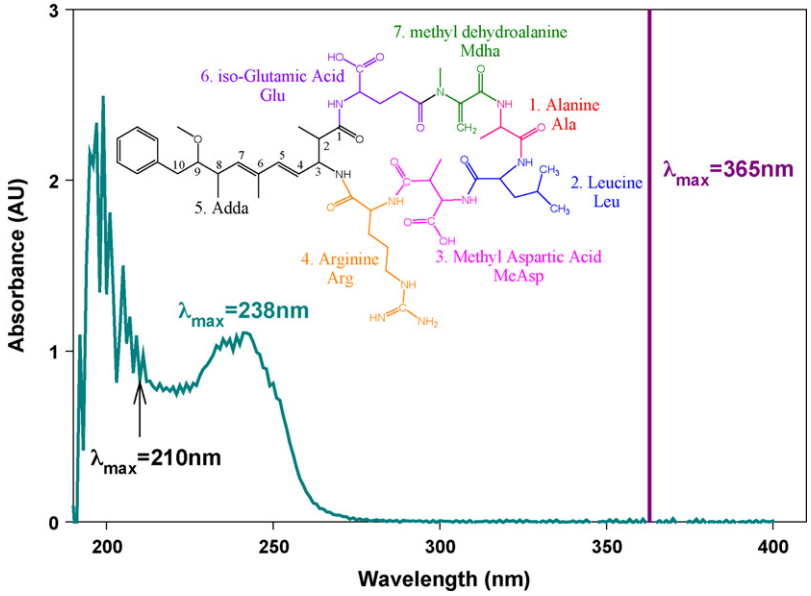

Fig. 2. The chemical structure and the UV–vis absorbance spectra of MC-LR in pH_{sq} = 5.7.

nanoparticles have used catalyst doses as high as two orders of magnitude (20–100 mg TiO_2) [16–18]. The results herein indicate that a small amount of catalyst is sufficient to remove high concentrations of the toxin. Even though other studies utilizing photocatalytic films have been reported in the literature [10,19,28] differences in the preparation method, film thickness and coated area do not allow for direct comparison with the results presented here. The advantages of using this preparation method compared with the others include (a) the deposition of a thin layer of catalyst (0.1 μm) onto the substrate after each dip-coating/calcination cycle allows versatility of usage (films and membranes), (b) the fabrication of thin, transparent photocatalytic films which allow light penetration and simultaneous activation of both coated sides, and (c) synthesis of mechanically stable crack-free films, with high photocatalytic activity because of the optimum crystallite size (9.2 nm) [22].

3.2. Effect of initial solution pH

To determine the effect of pH on the degradation of MC-LR, toxin solutions with initial concentration of C_o = 2000 μg/L (~2.0 μM) at acidic and neutral pH were tested. The degradation was first conducted in Milli-Q water (pH_{sq} = 5.7) as a control to account for the effects of counter-ions in the buffered/adjusted experiments. For acidic pH_o = 3.0 the solution was adjusted with 5N H_2SO_4 while for neutral pH_o = 6.82, buffered (0.025 M K_2HPO_4 and 0.025 M KH_2PO_4) and solutions adjusted with 0.1N NaOH and 5N H_2SO_4, were used. Fig. 3 presents the toxin concentration profiles with the acidic pH exhibiting the fastest rate of degradation. As discussed in previous publications [9,10,17], the preferential pH for the degradation and adsorption of MC-LR into porous titania is around pH 3.5 because of the attractive forces forming between the positively charged titania ($TiOH_2^+$) and the negatively charged toxin ($MCLRH^-$) [Eqs. (1) and (2)]. Since hydroxyl radicals are formed on the catalyst surface ($HO_{surf}^{\bullet}$) [29] these attractions between the contaminant and the catalyst increase the utilization rate of $HO^{\bullet}$ and therefore enhance the degradation rate of MC-LR.

$$> TiOH_2^+ \xrightarrow{-H^+ [pKa_1=2.6]} \underset{(PZC \approx 6.4)}{> TiOH} \xrightarrow{-H^+ [pKa_2=9.0]} > TiO^- \quad (1)$$

$$\underset{(+)}{MCLRH_3^+} \underset{pk_1=3.0}{\leftrightarrow} \underset{(0)}{MCLRH_2^\circ} \underset{pk_2=3.0}{\leftrightarrow} \underset{(-1)}{MCLRH^-} \underset{pk_3=12.5}{\leftrightarrow} \underset{(-2)}{MCLR^{2-}} \quad (2)$$
$$\xrightarrow[pH]{}$$

The efficiency of MC-LR degradation at neutral pH (buffered, unbuffered, adjusted) appears to be independent of phosphate and sulfate anions in the matrix (Fig. 3). Statistical analysis of

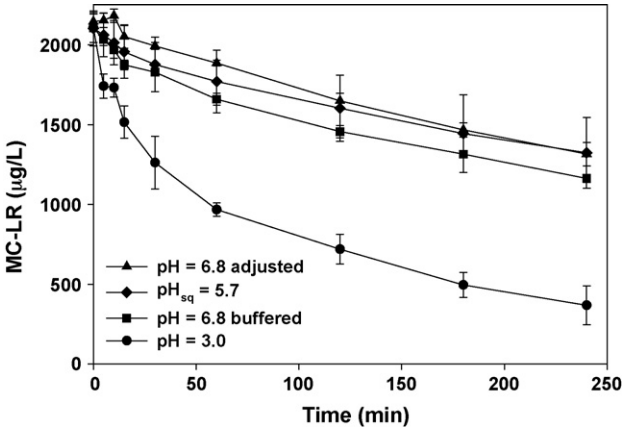

Fig. 3. Degradation of 2000 μg/L of MC-LR, with thin films at pH = 3.0 and pH = 6.82.

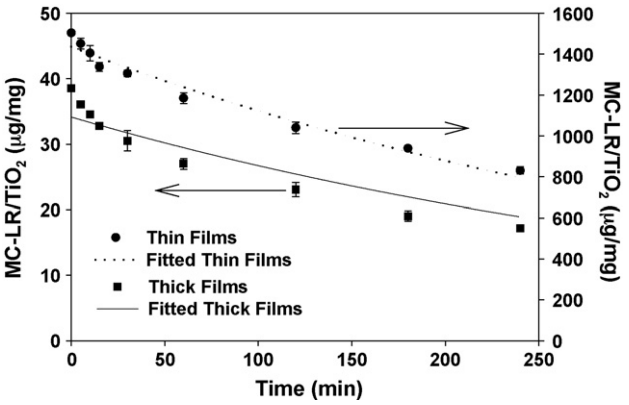

Fig. 4. Comparison of the degradation efficiencies of thin and thick films at buffered solutions (pH_o = 6.82).

individual points (t = 0, 30, 60, 120 and 240 min) from the three experiments were analyzed with one-way ANOVA combined with Bonferroni's test and were found to be statistically not different ($0.13 \leq P \leq 0.99$). Therefore, the counter-ions in the solution have no significant effect on the degradation of MC-LR at neutral pH. This conclusion is also in agreement with prior studies (i.e. Dionysiou et al, 2001; Pichat et al., 1993) that found phosphate and sulfate ions do not inhibit the photocatalytic degradation of aromatic compounds at pH values higher than the point of zero charge of the titania (PZC_{TiO2}~6.4) [30,31].

Thick photocatalytic films (6.7 μm) prepared by dip-coating stainless steel plates into an alkoxide sol–gel modified with colloidal TiO_2 nanoparticles were also tested previously for the degradation of MC-LR [10]. At acidic pH = 3.0 and under the same experimental conditions (treated volume, initial concentration, radiation type and intensity) degradation of the toxin was completed in 30 min with the thick films. Since significantly higher amount of catalyst is immobilized on the stainless steel (50.4 mg TiO_2) compared to the glass plate (1.4 mg TiO_2) longer treatment times with the thin films were expected. However, when MC-LR was degraded in separate buffered solutions (pH = 6.82) for the thin and thick films, the degradation efficiencies, after 4 h of treatment, were surprisingly comparable (45 and 55% MC-LR removal, respectively). Statistical analysis of the normalized concentration of MC-LR with same amount of catalyst for each film versus time [$(mass_{MCLR}/mass_{TiO2}) = F(time)$] (Fig. 4) shows that the k constants for the two films are not statistically different (P = 0.86). This is because at neutral pH, strong interactions between MC-LR and the catalyst are replaced by weaker momentary forces such as *van der Waals*, and the destruction of the toxin most probably occurs by the hydroxyl radicals that diffuse in the bulk of the solution and attack the toxin molecules that are close to the catalyst's surface.

3.3. Effect of initial concentration

The concentration of cyanotoxins in water resources can very from ng/L to mg/L depending on the type, density and persistence of the bloom [4,32–34]. Therefore it was imperative to test the efficiency of the photocatalytic films to degrade cyanotoxins at a wide range of concentrations. MC-LR solutions ranging from 830 to 5355 μg/L (0.84–5.38 μM) were used to determine the effects of initial concentration (Fig. 5). Based on the previous discussion, the remaining experiments were performed in acidic pH unless noted otherwise. The photocatalytic degradation of MC-LR follows *pseudo-first order* kinetics. The dependency of the reaction rate (dC/dt) on concentration was confirmed by its steady increase with an increasing initial toxin concentration

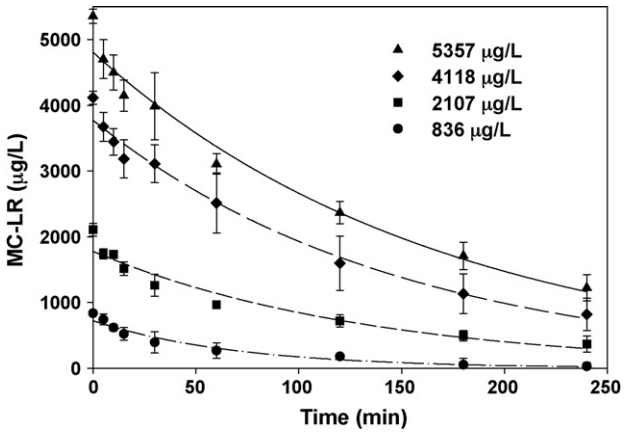

Fig. 5. Degradation of MC-LR with thin films at different initial concentrations, pH_o = 3.0.

Table 1
Initial rates of degradation of MC-LR at pH = 3.0.

Initial Concentration (μM)	Initial rate × 10^{-2}(μM/min)
0.84	1.48
2.12	2.81
4.14	3.23
5.38	3.82

(Table 1). Langmuir-Hinshelwood (L-H) is the most applied kinetic model for fitting data from photocatalytic degradation [17–19,25,35–37] because of its goodness of fitting [38].

Many studies have found that the K_{ads} from the L-H model is orders of magnitude smaller compared to the constant from dark adsorption isotherms [18,19,39]. This difference has been attributed to changes of the electric properties of TiO_2 surface upon irradiation which possibly affect the distribution adsorption sites and the dependency of K_{ads} on light intensity [39,40]. However, a recent article has raised concerns about the applicability of the L-H model to universally describe photoprocesses in heterogeneous systems [38]. Part of the requirements of the L-H model includes the physiosorption of reactants on the catalyst in a monolayer, only one adsorbate being involved per active site. In the case of MC-LR, it is reported that one toxin molecule can occupy up to 5 active sites of TiO_2 because of its size and 3-D structure [17]. Because of discrepancies with the requirements of L-H model and the possibility of MC-LR chemically reacting with the TiO_2 surface (more explanation in the following section) the L-H model may not describe the photocatalytic degradation of MC-LR presented herein (even though theoretically, it does fit our data well). Instead we report here the photocatalysis of MC-LR follows *pseudo-first order* kinetics for the range of concentrations studied.

3.4. Effect of film surface area (thin films)

In order to increase the degradation rate of MC-LR, the toxin at an initial concentration of 2000 μg/L (~2.0 μM), was treated with 1, 2, and 3 films (Fig. 6a). By increasing the number of films in the reactor, the contact surface area between the water and the catalyst is increased. The contact surface area is a critical parameter as the hydroxyl radicals are formed and react primarily on the surface of the catalyst and to a lesser extends in the bulk of the solution [10,18]. The initial rate of MC-LR degradation (averaged at 30 min) increased with surface area as $r_1 = (2.82 \pm 0.31) \times 10^{-2}$ mM/min; $r_2 = (4.20 \pm 1.1) \times 10^{-2}$ mM/min; $r_3 = (5.38 \pm 0.53) \times 10^{-2}$ mM/min. Feitz et. al. (1999), proposed that at acidic pH a stoichiometric complexation

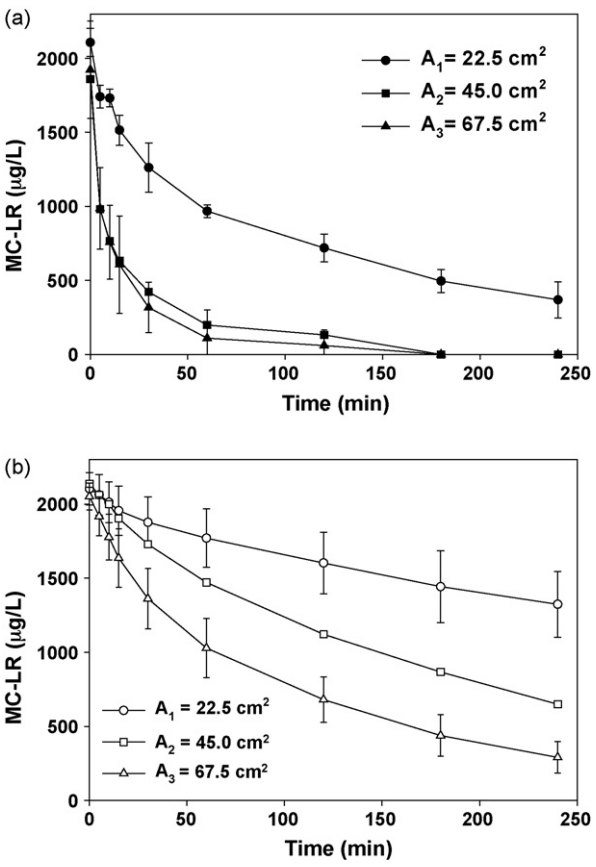

Fig. 6. (a) Effect of the film surface area on the degradation of 2000 μg/L of MC-LR at pH = 3.0. (b) Effect of the film surface area on the degradation of 2000 μg/L of MC-LR at pH_{sq} = 5.7.

reaction ($Kc = 10^8$) takes place between MC-LR and the surface of TiO_2 for the formation of a neutral complex (>TiMCLRH) [17]. In case of one film, the degradation was limited by the availability of TiO_2 sites for complexation with MC-LR. But when two and three films were used the concentration of MC-LR was not enough to cause saturation of the TiO_2 surface making the toxin concentration the limiting factor. The differences in the limiting factors between single and multi films contributed to the non-linear relationship between the initial rates of degradation and the film surface area.

Since at neutral pH the complexation reaction is not as dominant as in acidic pH, the degradation is based mainly on the radicals that escape the surface of the catalyst and diffuse in the bulk of the solution. In this case, the initial rate of MC-LR degradation (averaged at 30 min) increased with surface area as $r_1 = (0.64 \pm 0.3) \times 10^{-2}$ mM/min; $r_2 = (1.72 \pm 0.65) \times 10^{-2}$ mM/min; $r_3 = (2.31 \pm 0.45) \times 10^{-2}$ mM/min (Fig. 6b).

3.5. Effect of film thickness and porous structure

Changes in the morphology of the catalyst can impact the number of active sites, transportation of reagents/products to and from the catalytic sites, the activation energy of the catalyst, as well as the generation and recombination rates of the electron-hole pairs [22]. At first, the optimum number of dip-coating layers was investigated since film thickness affects the adsorption capacity of the catalyst hence the photocatalytic activity, the mechanical stability of the films and manufacturing cost [22,23,41]. Photocatalytic films prepared by increasing the dip-coating/calcination cycles (T = 1, 3, 5, and 10), were placed in reactor vessels with Milli-Q water solutions for an hour to test for

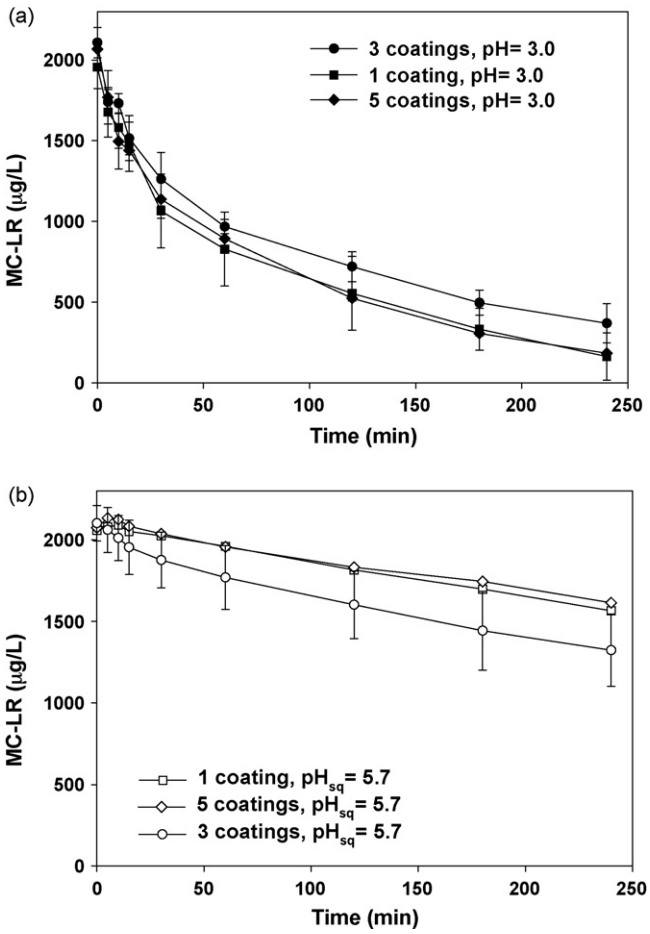

Fig. 7. (a) Effect of the film thickness on the degradation of 2000 μg/L of MC-LR at pH = 3.0. (b) Effect of the film thickness on the degradation of 2000 μg/L of MC-LR at pH_{sq} = 5.7.

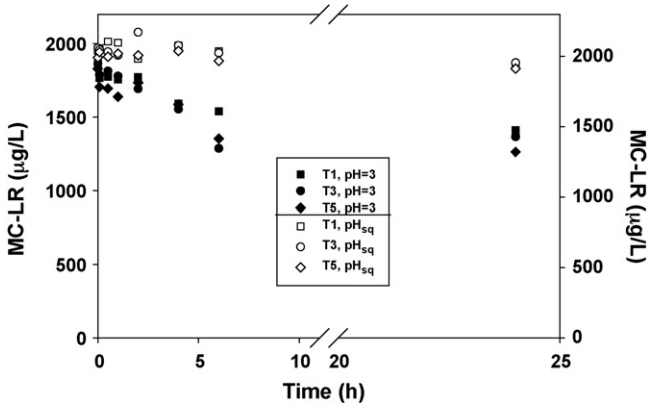

Fig. 8. Dark adsorption of MC-LR at acidic and neutral pH over a 24-h period with films of different thickness.

their mechanical stability. Flaking of the catalyst was observed after T = 10 calcination cycles and therefore, these films were not used for the degradation of MC-LR. As seen in Fig. 7a, the degradation efficiencies of MC-LR were the same irrespective of the number of layers. Statistical analysis with global fitting found the k constants to be not different (P = 0.22). In an earlier study where methylene blue (MB) was used as the model contaminant, the degradation efficiency increased with increasing layers until T = 3 and then reached a plateau for T = 5, 7, 9. Since the photocatalytic films are thin enough to allow light penetration and catalyst activation of the inner layers, it is presumed that only the three outer layers are actively participating in the photocatalytic degradation processes [22]. We did not see the same behavior for MC-LR possibly because of differences in the size and the chemical structure of the two compounds. MB is a significantly smaller molecule (FW 319.9, diameter 1.0 nm) than MC-LR (FW 995.2, diameter 2.4 nm) and can penetrate and move more easily between the coating layers, increasing its adsorption capacity in the films and consequently its degradation rate. To test the hypothesis whether MC-LR can penetrate into the inner layers of the thin films given enough contact time, dark adsorption studies with T = 1, 3, and 5 at acidic and neutral and C_{MCLR}~2 μM were conducted (Fig. 8). Samples were taken at predetermined time intervals for 24 h. Adsorption of MC-LR at neutral pH was not observed while at acidic pH it was complete within 4 h, reaching a plateau thereafter. At the end of 24 h, ~5.0 nmol of MC-LR was adsorbed in each film irrespective of the film thickness. Based on these results, it does not appear that MC-LR can penetrate significantly through the inner layers of films and the adsorption as the degradation takes place only in the outer layer. Thus, the degradation efficiencies of MC-LR at acidic pH are independent of film thickness Fig. 7a. Another possible explanation would be that the initial toxin molecules, which strongly adsorb in the mesopores, because of the attractive forces developed between the negatively charged toxin and positively charged titania, block the passage for the remaining molecules and inhibit penetration of the toxin towards the inner layers (pores range is 3–7 nm). When films with macropores were used in a previous study, the toxin penetrated towards the inner layers at acidic pH [10]. Scheme 1a and b depict two possible ways that MC-LR interacts with the surface of the catalyst, exposing each time different moieties of the toxin for degradation. In the first case, the cyclic structure of the toxin is found inside the pore while the ADDA chain expands away from the catalyst's surface, exposing the unsaturated bonds of the Mdha amino acid to HO• attack (Scheme 1a). Another possibility is for the entire toxin to enter the pore exposing to HO• attack the functional groups (aromatic ring, methoxy group and diene bonds) consisting the ADDA chain as well (Scheme 1b) [11].

The same degradation experiment (film thickness) was repeated in Milli-Q water, and as expected, the degradation efficiencies of MC-LR were significantly lower compared to acidic pH. However, the degradation with the T = 3 was faster than T = 1, 5 (Fig. 7b). For T = 1 it is believed that the amount of catalyst is not sufficient to utilize all the light intensity for activation and the rate of HO• production is lower than in T = 3, 5. At T = 5 even though the inner layers are activated by radiation, mass transfer limitations prohibit the escape of radicals in the bulk of the solution (were the majority of the toxin is) and degrade it. Based on these results it was decided to use T = 3 as the optimum layers for the films.

Further investigations of the combined effects of film's surface properties and pH, were conducted by modifying the preparation method and testing the resulting films at acidic and neutral pH. A critical component of this preparation method is the non-ionic surfactant (Tween 80, Sigma) used as templating material to customize the porosity to the mesoporous range and enhance the surface properties of the films. The control films were prepared without the surfactant, exhibiting non-porous structure with low BET surface area of 22.7 m^2/g and porosity of 12.6%, while the crystal size was not significantly affected (12.4 nm) [23]. As shown in Fig. 9, the TiO_2 films showed increased photocatalytic activity up to 10% and 15% at pH 5.7 and 3.0 compared to control films, respectively, even though the control films have ~25% more catalyst/cm^2 (88.4 μg/cm^2). The non-porous structure of the control films reduced the contact area between the surface of the catalyst and the toxin solution, as well as the adsorption of MC-

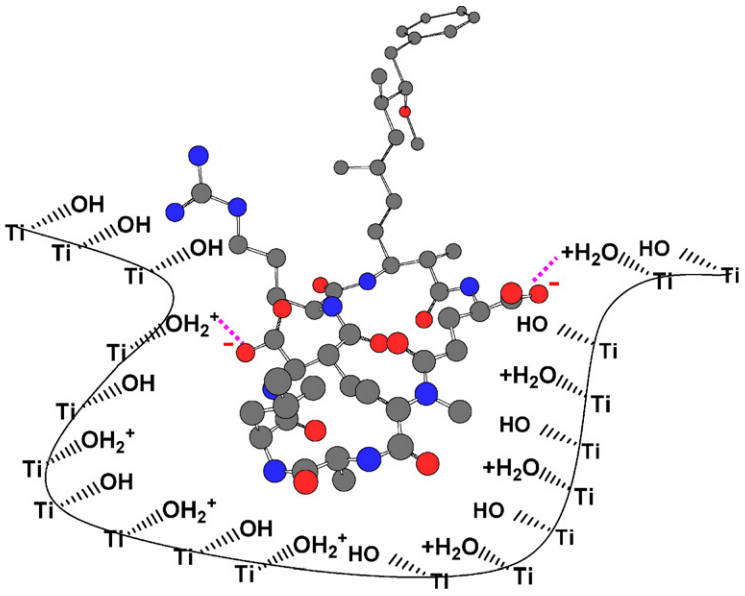

(a) $HO^{\bullet}$ attack on the cyclic structure of MC-LR

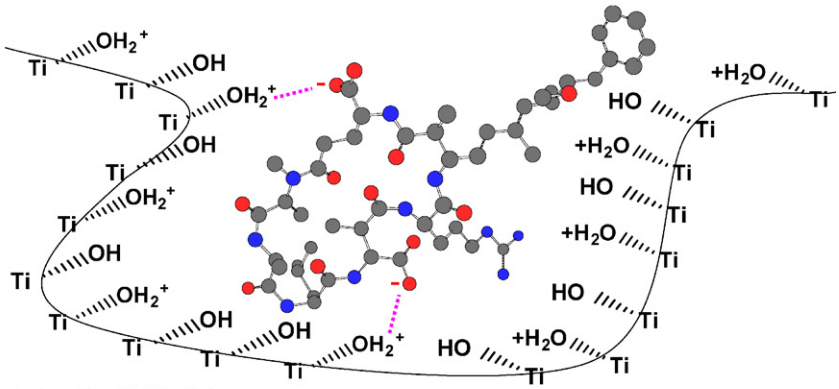

(b) $HO^{\bullet}$ attack on the ADDA chain

Scheme 1. Interactions of MC-LR with TiO_2 at acidic conditions. (a) $HO^{\bullet}$ attack on the cyclic structure of MC-LR. (b) $HO^{\bullet}$ attack on the ADDA chain.

LR onto and into the films. On the other hand, the control films maintained their crystal structure and the crystallite size was close to the optimum range (8–10 nm) for high photocatalytic activity [22]. It is believed that this was the major reason that the control films resulted in ~65% removal of the initial toxin concentration after 4 h of treatment. Also the results in Fig. 9 reinforce the importance of substrate adsorption and interactions controlled by the solution pH. Fig. 9 also suggests that pH is the dominant parameter that controls the efficiency of this process, since the control film at pH 3.0 performed better than the film prepared with the surfactant at pH 5.7.

3.6. Detoxification studies

The hepatotoxic nature of microcystins is partially attributed to their ability to inhibit the function of important enzymes, protein phosphatases (PP), in the cell. PPs are responsible for the dephosphorylation of various proteins in a cell. Since protein phosphorylation/dephosphorylation governs a large number of cellular processes (such as cell-cycle progress, cell proliferation, protein synthesis, transcriptional regulation and neurotransmission) PPs play an important role in the maintenance of cellular function and survivability [42].

Because MC-LR has been reported to be a potent inhibitor of PP1, the toxicity of the treated samples was assessed using a colorimetric assay that measures the activity of PP1. In particular, when PP1 is incubated (37 °C) with the phospho-substrate p-nitrophenyl phosphate (pNPP), it releases phosphoric ions and the colorimetric compound, p-nitrophenol (green color). The production of the p-nitrophenol and consequently the activity of PP1 can be quantified by measuring the solution absorption at λ = 405 nm. This assay was optimized for the enzyme (0.0025 mg/mL) and substrate (40 mM pNPP) concentrations and reaction time (30 min). Standard solutions of MC-LR (1–2000 μg/L, pH = 3.0) were used to form the inhibition curve of the toxin with the PP1 enzyme (Fig. 10). In our hands, the 50th percentile of PP1 inhibition (IC_{50}) was determined at 157.5 μg/L of MC-LR. Previous studies reported that the IC_{50} is between 0.3 and 38 μg/L [43–47]. These discrepancies may be related to the enzyme concentration, isoform used and sensitivity of the assay. It has been consistently reported that increasing the enzyme concentration, causes significant increases in the IC_{50} [43,47]. Nevertheless, we were working under linear range conditions which enabled us to use this method and assess the toxicity of the photocatalytically treated samples.

Based on results from experiments on the coated surface area of the films (A = 67.5 cm^2, pH = 3.0), select samples treated at times t

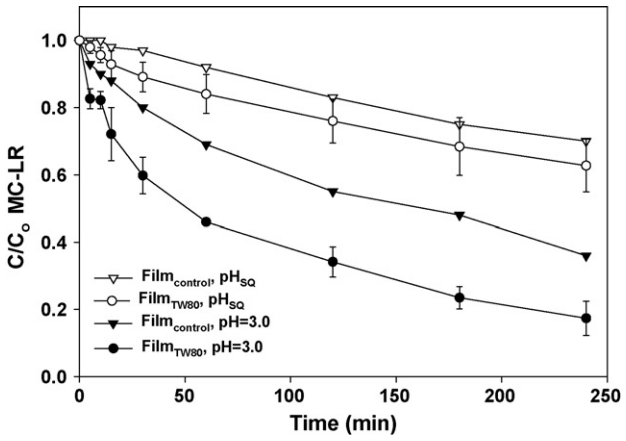

Fig. 9. The effect of surfactant (film preparation): degradation of 2000 μg/L of MC-LR with control film and regular films at acidic and neutral pH.

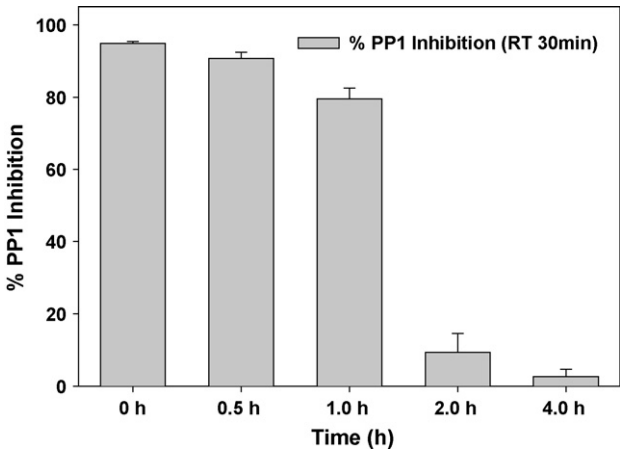

Fig. 11. Percentage of PP1 inhibition of samples following TiO_2 treatment at different time intervals.

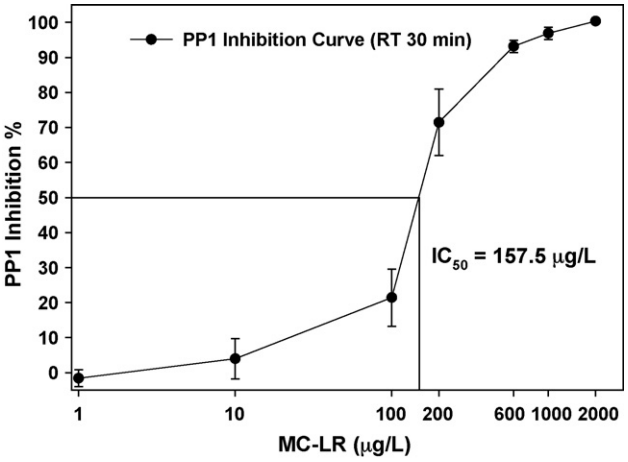

Fig. 10. PP1 Inhibition Curve of MC-LR ($1.0 \leq C_{MCLR} \leq 2000$ μg/L; 30 min reaction time).

=0, 0.5, 1.0, 2.0 and 4.0 h were analyzed with the PP1 assay (Fig. 11). After 1 h of TiO_2 photocatalytic treatment, ~80% of PP1 is inhibited, which is consistent with the remaining toxin concentration at that time (~300 μg/L) (Fig. 6a, Fig. 10). Besides the residual MC-LR, the potential toxicity of primary intermediates may possibly account for the high inhibition. We have extensively studied the transformations of MC-LR during treatment with TiO_2 photocatalytic films in a previous publication and after analyzing the obtained LC/MS data, found that two sets (Set 1 and Set 2) of intermediates are formed during treatment with TiO_2 photocatalytic films which gave peak area maxima at the 1–2 h and 2–3 h of treatment [11]. The first set (Set 1) of identified intermediates showed subtle alterations like hydroxylation (through substitution or addition) of the unsaturated bonds of the toxin and oxidation of the methoxy functional group. However, in the second set (Set 2) of intermediates more drastic changes occurred, such as cleavage of the methoxy group, complete removal of the side chain of the ADDA moiety and destruction of the cyclic structure (Figs. 2 and 12). In Fig. 12 the peak areas of intermediates involved in three distinct degradation pathways of MC-LR: aromatic ring hydroxylation (m/z 1011.5 and 1027.5), removal of methoxy group (m/z 1009.5 and 965.5) and hydroxylation of the diene bonds of ADDA moiety (m/z 1029.5 and 1063.5) are shown. For some of these intermediates i.e., 6(Z)-MC-LR and the demethoxylated-MC-LR (DmADDA) studies [11,48,49] indicated that they possess no toxicity. For others such as the hydroxylated and isomerized diene bonds there is speculation of reduced or no toxicity because of changes in the hydrophobicity and orientation of the ADDA chain that possibly hinders them from properly binding with the PP1 enzyme [42,50,51]. Towards the end of the treatment, the structure of MC-LR was significantly degraded (destruction of cyclic structure and removal of the hydrophobic chain) [11] and no PP1 activity inhibition is expected. Indeed, as the photocatalytic degradation progressed, the inhibition decreased significantly after 2 h of treatment (~10%) and by 4 h, the enzyme activity recovered completely. The observed

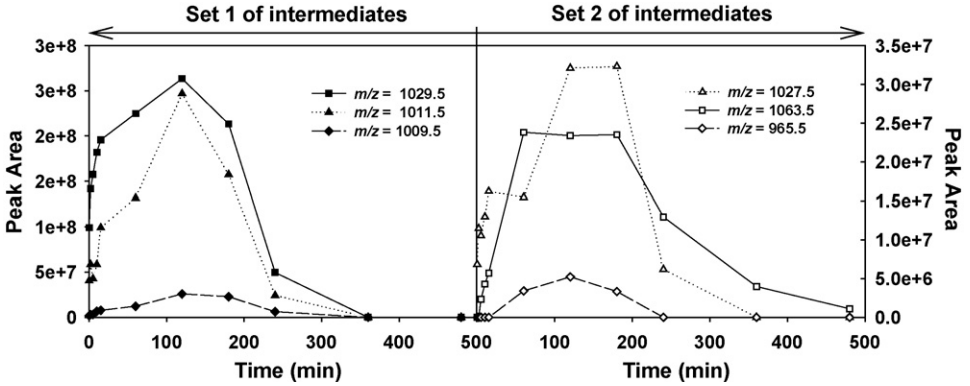

Fig. 12. Peak area profiles (from LC/MS data) of select MC-LR intermediates from the Set 1 and Set 2 that participate in three different degradation pathways (▲: aromatic ring; ◆: methoxy group; ■: diene bonds).

decrease in toxicity supports that the subsequent intermediates/products of MC-LR have significantly lower toxicity or possess no toxicity. Similar results were observed by Liu et al. (2002) using TiO_2 in suspension [16].

4. Conclusion

In this study, thin transparent TiO_2 photocatalytic films immobilized on glass plates were tested for the degradation of an emerging drinking water contaminant, MC-LR. Significant amount of the toxin was retained at the surface of the catalyst because of the structural properties of the films and solution pH. Toxin degradation was observed only when both irradiation and the catalyst were present. Increasing film thickness did not enhance the degradation most probably because of mass transfer limitations for the toxin to reach and react with the inner layers of the catalyst. The absence of pore-shaping surfactant caused a 15% decrease in the performance of films. Increasing the contact area between the liquid and the catalyst enhanced the degradation rates even at the sub-optimum degradation at neutral pH. This means that a more efficient reactor design can counteract the unfavorable effects induced by solution pH and mass transfer. Detoxification studies based on the inhibition of the PP1 enzyme indicated complete loss of the toxic effects of MC-LR following photocatalytic treatment. These results suggest that utilization of thin TiO_2 photocatalytic films may be an efficient technology for detoxification of microcystin-contaminated water.

Acknowledgments

This research was funded in part by the National Science Foundation through a CAREER Award (BES-0448117) to D.D.D., the U.S.EPA (RD-83322301) and the Center of Sustainable Urban Engineering (SUE) at the University of Cincinnati. M.G.A. is grateful to *Sigma Xi*, The Scientific Society for a Grant-in-Aid of Research Fellowship, the Rindsberg Memorial Fund of UC and the University Research Council of UC for a Summer Research Fellowship. M.G.A. is also thankful to Shirish Agarwal (UC) and Hyeok Choi (USEPA) for insightful input.

Disclaimer: Although this work was reviewed by EPA and approved for publication, it may not necessarily reflect official Agency policy.

References

[1] M.G. Antoniou, A.A. de la Cruz, D.D. Dionysiou, Journal of Environmental Engineering 131 (2005) 1239–1243.
[2] W.W. Carmichael, Scientific American 270 (1994) 78–86.
[3] W.W. Carmichael, Journal of Applied Bacteriology 72 (1992) 445–459.
[4] C.M. Cook, E. Vardaka, T. Lanaras, Acta Hydrochimica et Hydrobiologica 32 (2004) 107–124.
[5] Y. Xie, Z. Xiong, G. Xing, X. Yan, S. Shi, G. Sun, Z. Zhu, Atmospheric Environment 42 (2008) 5182–5192.
[6] China vows to clean up polluted lake, Retrieved May 11, 2009, from: http://www.nytimes.com/2007/10/27/world/asia/27china.html?scp=2&sq=Lake+tai&st=nyt.
[7] S. Yu, N. Zhao, X. Zi, Chinese Journal of Oncology 23 (2001) 96–99.
[8] Australian Drinking Water Guidelines, Retrieved May 11, 2009, from: http://www.nhmrc.gov.au/publications/synopses/_files/adwg_11_06.pdf.
[9] H. Choi, M.G. Antoniou, M. Pelaez, A.A. De La Cruz, J.A. Shoemaker, D.D. Dionysiou, Environmental Science and Technology 41 (2007) 7530–7535.
[10] M.G. Antoniou, J.A. Shoemaker, A.A. de la Cruz, D.D. Dionysiou, Toxicon 51 (2008) 1103–1118.
[11] M.G. Antoniou, J.A. Shoemaker, A.A. De La Cruz, D.D. Dionysiou, Environmental Science and Technology 42 (2008) 8877–8883.
[12] L.A. Lawton, P.K.J. Robertson, Chemical Society Reviews 28 (1999) 217–224.
[13] J. Lee, H.W. Walker, Environmental Science and Technology 40 (2006) 7336–7342.
[14] W. Schmidt, H. Willmitzer, K. Bornmann, J. Pietsch, Environmental Toxicology 17 (2002) 375–385.
[15] M.R. Hoffmann, S.T. Martin, W. Choi, D.W. Bahnemann, Chemical Reviews 95 (1995) 69–96.
[16] I. Liu, L.A. Lawton, B. Cornish, P.K.J. Robertson, Journal of Photochemistry and Photobiology A: Chemistry 148 (2002) 349–354.
[17] A.J. Feitz, T.D. Waite, G.J. Jones, B.H. Boyden, P.T. Orr, Environmental Science and Technology 33 (1999) 243–249.
[18] P.K.J. Robertson, L.A. Lawton, B. Münch, J. Rouzade, Chemical Communications (Cambridge) 1994 (1997) 393–394.
[19] P.K.J. Robertson, L.A. Lawton, B. Münch, B. Cornish, Journal of Advanced Oxidation Technologies 4 (1999) 20–26.
[20] G.S. Shephard, S. Stockenström, D. De Villiers, W.J. Engelbrecht, E.W. Sydenham, G.F.S. Wessels, Toxicon 36 (1998) 1895–1901.
[21] G.S. Shephard, S. Stockenström, D. De Villiers, W.J. Engelbrecht, G.F.S. Wessels, Water Research 36 (2002) 140–146.
[22] H. Choi, E. Stathatos, D.D. Dionysiou, Applied Catalysis B: Environmental 63 (2006) 60–67.
[23] H. Choi, E. Stathatos, D.D. Dionysiou, Thin Solid Films 510 (2006) 107–114.
[24] T.C. Long, N. Saleh, R.D. Tilton, G.V. Lowry, B. Veronesi, Environmental Science and Technology 40 (2006) 4346–4352.
[25] B. Boulinguiez, A. Bouzaza, S. Merabet, D. Wolbert, Journal of Photochemistry and Photobiology A: Chemistry 200 (2008) 254–261.
[26] M. Welker, C. Steinberg, Environmental Science and Technology 34 (2000) 3415–3419.
[27] W. Song, S. Bardowell, K.E. O'Shea, Environmental Science and Technology 41 (2007) 5336–5341.
[28] X. Feng, F. Rong, D. Fu, C. Yuan, Y. Hu, Chinese Science Bulletin 51 (2006) 1191–1198.
[29] R. Nakamura, Y. Nakato, Journal of the American Chemical Society 126 (2004) 1290–1298.
[30] D.D. Dionysiou, M.T. Suidan, I. Baudin, J.M. Lainé, T.L. Huang, Water Science and Technology: Water Supply 1 (2001) 139–147.
[31] P. Pichat, C. Guillard, C. Maillard, L. Amalric, J.C. D'Oliveira, Photocatalytic Purification and Treatment of Water and Air (1993) 207–223.
[32] J.L. Sinclair, S. Hall, J.A. Berkman, G. Boyer, J. Burkholder, J. Burns, W. Carmichael, A. DuFour, W. Frazier, S.L. Morton, E. O'Brien, S. Walker, Advances in Experimental Medicine and Biology 619 (2008) 45–103.
[33] G.J. Jones, P.T. Orr, Water Research 28 (1994) 871–876.
[34] C.M. McDermott, R. Feola, J. Plude, Toxicon 33 (1995) 1433–1442.
[35] M.G. Antoniou, D.D. Dionysiou, Catalysis Today 124 (2007) 215–223.
[36] E. Stathatos, K. Pelentridou, H. Karasali, D.D. Dionysiou, P. Lianos, International Journal of Photoenergy (2008).
[37] H. Al-Ekabi, N. Serpone, E. Pelizzetti, C. Minero, M.A. Fox, R.B. Draper, Langmuir 5 (1989) 250–255.
[38] N. Serpone, Journal of Advanced Oxidation Technologies 10 (2007) 111–115.
[39] S. Parra, S.E. Stanca, I. Guasaquillo, K. Ravindranathan Thampi, Applied Catalysis B: Environmental 51 (2004) 107–116.
[40] Y. Xu, C.H. Langford, Journal of Photochemistry and Photobiology A: Chemistry 133 (2000) 67–71.
[41] H. Choi, M.G. Antoniou, A.A. de la Cruz, E. Stathatos, D.D. Dionysiou, Desalination 202 (2007) 199–206.
[42] J. Goldberg, H. Huang-b, Y. Kwon-g, P. Greengard, A.C. Nairn, J. Kuriyan, Nature 376 (1995) 745–753.
[43] W.W. Carmichael, J. An, Natural Toxins 7 (1999) 377–385.
[44] J. An, W.W. Carmichael, Toxicon 32 (1994) 1495–1507.
[45] W. Song, T. Teshiba, K. Rein, K.E. O'Shea, Environmental Science and Technology 39 (2005) 6300–6305.
[46] C.J. Ward, K.A. Beattie, E.Y.C. Lee, G.A. Codd, FEMS Microbiology Letters 153 (1997) 465–473.
[47] R.E. Honkanen, J. Zwiller, R.E. Moore, S.L. Daily, B.S. Khatra, M. Dukelow, A.L. Boynton, Journal of Biological Chemistry 265 (1990) 19401–19404.
[48] S. Takenaka, Y. Tanaka, Chemosphere 31 (1995) 3635–3641.
[49] K. Tsuji, T. Watanuki, F. Kondo, M.F. Watanabe, S. Suzuki, H. Nakazawa, M. Suzuki, H. Uchida, K.I. Harada, Toxicon 33 (1995) 1619–1631.
[50] K.I. Harada, Toxic Microcystis (1996) 103–148.
[51] K.I. Harada, S. Imanishi, H. Kato, M. Mizuno, E. Ito, K. Tsuji, Toxicon 44 (2004) 107–109.